

## 3,4'-Bis[bis(*t*-butyl- and methoxy-phenyl)amino]stilbene Bis(cation radical)s and Their Electrochemical and Magnetic Properties

Tsuyoshi Michinobu, Eishun Tsuchida, and Hiroyuki Nishide\*

Department of Polymer Chemistry, Waseda University, Tokyo 169-8555

(Received August 30, 1999)

3,4'-Bis[bis(*p*-*t*-butylphenyl)amino]stilbene **1a** and 3,4'-bis[bis(*p*-methoxyphenyl)amino]stilbene **1b** were synthesized. The oxidation of **1** was analyzed by electrochemical measurements, which revealed the reversible formation of the bis(cation radical) **2** via a two-electron transfer reaction. The chemical oxidation of **1** with NOBF<sub>4</sub> also gave the bis(cation radical) **2**; UV/vis and ESR spectroscopies supported aminium radical formation without any side reaction. Magnetization, magnetic susceptibility, and the ESR  $\Delta M_s = \pm 2$  signal of the biradicals indicated triplet ground states with a large triplet-singlet energy gap.

An attempt to realize very high-spin organic molecules using intramolecular through-bond magnetic ordering has become of great interest.<sup>1,2</sup> Among them, many  $\pi$ -conjugated, but non-Kekulé type, biradical molecules have been prepared by taking into account their topological symmetry and spin polarization in their alternant conjugations.<sup>3</sup> While some of them succeeded in forming triplet ground-state molecules built in the  $\pi$ -conjugated skeleton, an important aspect of the triplet molecules depended on the spin sources. For example, the spin density of the triarylmethyl radical is delocalized into the  $\pi$ -conjugated skeleton, which enhances the exchange interaction between the two spins on the biradical molecules.<sup>3b,3d</sup> However, this spin density delocalization increases the radical reactivity of the sterically unprotected skeleton, which often leads to chemical destabilization of the molecules. On the other hand, the galvinoxyl radical, whose spin density is localized on the radical moiety, has a substantial chemical stability.<sup>3a</sup> However, the localized spin reduces the exchange interaction on their biradical molecules. Therefore, a spin source, which is to be introduced into the  $\pi$ -conjugated skeleton, should be carefully selected from the list of radical species in order to satisfy both the sufficient exchange interaction and chemical stability for the multiple radical molecules.

Cation radicals of tris(*p*-substituted phenyl)amines, such as **3** or the corresponding triphenylaminium radicals, are known as one of chemically persistent radicals which can be isolated under ambient conditions.<sup>4</sup> It is also known that the spin density of the triphenylaminium radicals is delocalized into the phenyl groups.<sup>4</sup> The bis- and tris(cation radical)s of the *m*-bis(diphenylamino)- and 1,3,5-tris(diphenylamino)benzenes have been studied to reveal their ground-state triplet and quartet.<sup>5</sup> More recent research on the bi- and triaminium radicals using the field-swept 2D electron spin transient nutation method more clearly described their triplet and quartet states and ferromagnetic coupling capability of the

*m*-phenylene and 1,3,5-benzenetriyl  $\pi$ -conjugations.<sup>6</sup> These papers indicated that the triphenylaminium cation radicals, which have both the chemical stability and an effective distribution of the spin density, are one of the promising spin sources for synthesizing very high-spin organic molecules.

To our knowledge, all of the triplet and quartet molecules based on the triphenylaminium cation radicals are the bis- and tris(cation radical)s connected to *m*-phenylene and the 1,3,5-benzenetriyl groups. Bushby et al. recently extended these bi- and triradicals into a networked polyarylamine polymer; its cation radical cross-conjugatively formed in the network backbone displayed a nonet ground state.<sup>7</sup> However, no bis-(cation radical), which is derived from the triphenylamines connected with  $\pi$ -conjugated skeletons other than *m*-phenylene and is able to be extended to a  $\pi$ -conjugated polymer bearing pendant radicals, has been previously studied.

In this paper, 3,4'-disubstituted stilbene was for the first time selected as a ferromagnetic skeleton to connect the cationic aminium radicals (IUPAC recommended name: ammoniumyl radical); 3,4'-bis[bis(*p*-*t*-butylphenyl)amino]stilbene **1a** and 3,4'-bis[bis(*p*-methoxyphenyl)amino]stilbene **1b** (Chart 1) were synthesized, of which bis-(cation radical)s are the dimer units of the poly(4-diphenylaminium-1,2-phenylenevinylene)s.<sup>8</sup> We describe the synthesis of **1**, the formation of the bis(cation radical)s **2**, and their magnetic properties.

### Results and Discussion

**Synthesis.** The diphenylamines **4** were prepared by a palladium-catalyzed arylation<sup>9</sup> of the aniline derivatives; BINAP was an effective ligand of palladium for the selective monoarylation to give **4** in high yield. The methyl group of 3-bromotoluene was modified to a vinyl group via benzylic bromination and the Wittig reaction.<sup>10</sup> The resulting 3-bromostyrene was coupled with 1-bromo-4-iodobenzene, which selectively proceeded at the iodo position using a catalyst of

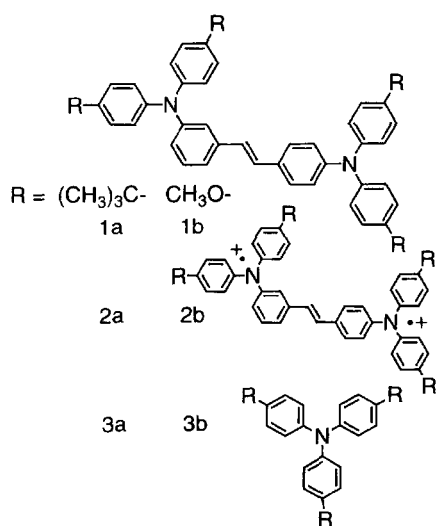


Chart 1.

palladium(II) acetate and tri-*o*-tolylphosphine to give 3,4'-dibromostilbene. The palladium-catalyzed amination of 3,4'-dibromostilbene with bis(*p*-*t*-butyl- or *p*-methoxy-phenyl)-amine, **4a** or **4b**, respectively, yielded 3,4'-bis[bis(*p*-*t*-butyl- or *p*-methoxy-phenyl)amino]stilbene, **1a** or **1b**, in a yield of more than 80%, which was higher than those from the preparation using Ullmann's copper chemistry (Scheme 1).<sup>11</sup>

The diaminostilbenes, **1a** and **1b**, were characterized by NMR spectroscopy. **1a** and **1b** possessed <sup>1</sup>H resonances in two regions, e.g., the aromatic moieties (7.4–6.7 ppm) and *t*-butyl (1.3 ppm) or methoxy groups (3.8 ppm), respectively. The aromatic regions were analyzed with the help of <sup>1</sup>H-<sup>1</sup>H COSY, HMQC, and HMBC experiments using the example of **1b**. The <sup>1</sup>H-<sup>1</sup>H COSY spectrum (Fig. 1) clearly resolved the complex <sup>1</sup>H NMR signals in the aromatic region, which showed four sets of phenylene rings and a set of off-diagonal resonances attributed to the vinylene unit (Fig. 1). HMQC and HMBC also substantiated the assignment and clarified the correlation of the <sup>13</sup>C NMR signals (see Experimental). The <sup>13</sup>C DEPT/NMR spectra were analyzed by comparing the numbers of expected and measured resonances in distinct spectral regions (e.g., aromatics). The diaminostilbenes, **1a** and **1b**, which lacked elements of symmetry in the aromatic regions, contained 24 and 21 nonequivalent carbon atoms, respectively. The exact assignments of the methyl, methine, and the quaternary carbons were accomplished by the combination of an approximation based

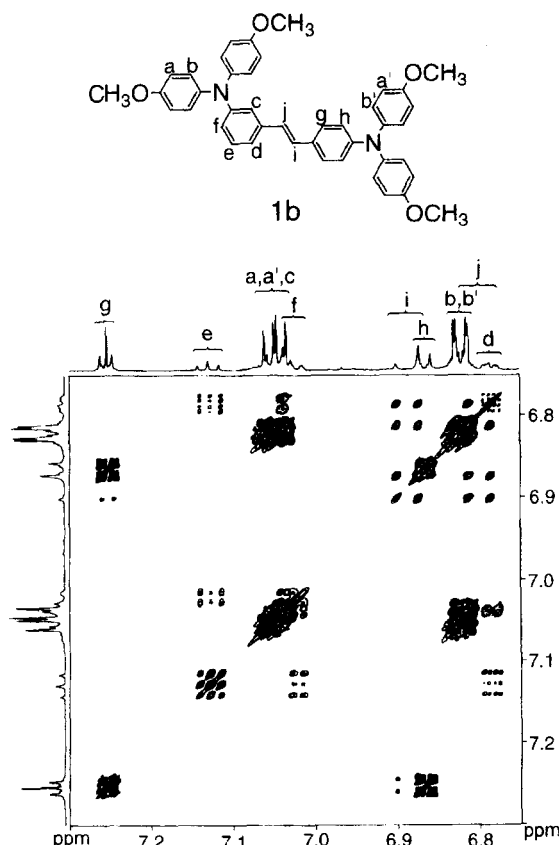
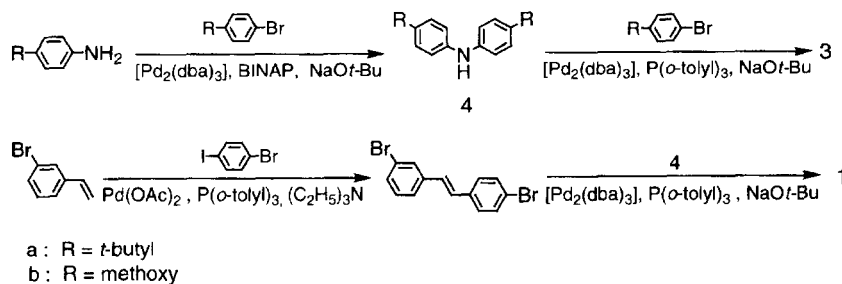


Fig. 1. <sup>1</sup>H-<sup>1</sup>H COSY correlation (600 MHz, CDCl<sub>3</sub>) in the aromatic region of the diaminostilbene **1b**.

on the additive law in the HMQC and HMBC spectra. The <sup>13</sup>C DEPT experiment of **1b** revealed a total of 21 carbon signals, of which one was attributed to the methyl, twelve to the methine, and eight to the quaternary carbons; these were consistent with the molecular structure. The *trans*-stilbene structure was supported by a strong fluorescence at 460 nm ( $\lambda_{\text{ex}} = 378$  nm) and 490 nm ( $\lambda_{\text{ex}} = 375$  nm) for **1a** and **1b**, respectively, and IR absorption at  $\delta_{\text{HC=CH}} = 960$  cm<sup>-1</sup>.

**Electrochemical Study.** The diaminostilbenes, **1a** and **1b**, displayed complete reversible redox waves during cyclic voltammetry (Fig. 2). The cation radicals **2** were stable in solution even at room temperature on the time scale of the voltammetry experiment. Compounds **3** also showed reversible redox waves; however, triphenylamine gave only a simple oxidation wave. The chemical stability of **1** in the redox reaction is considered to be realized by the introduction



Scheme 1.

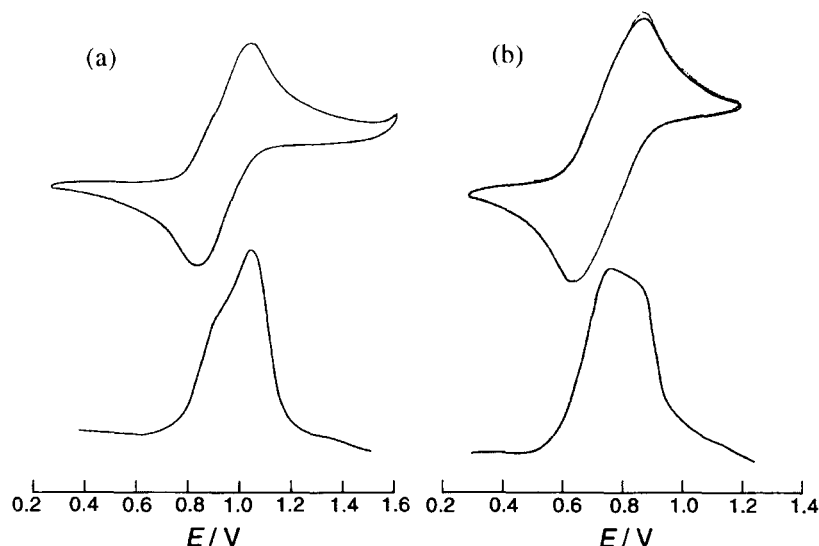


Fig. 2. Cyclic voltammograms and differential pulse voltammograms for **1a** (a) and **1b** (b) in  $\text{CH}_2\text{Cl}_2$  with 0.1 M  $(\text{C}_4\text{H}_9)_4\text{NBF}_4$  as a supporting electrolyte, at room temperature.

of the *p*-substituents, which prevent dimerization to form benzidine derivatives. The redox potentials (vs. Ag/AgCl), 0.93 and 0.75 V for **1a** and **1b**, respectively, were anodically shifted relative to those of the corresponding *p*-substituted triphenylamines, 0.89 and 0.65 V for **3a** and **3b**, respectively. The potentials were also explained by the electron-donating effect of the *t*-butyl and methoxy groups. The potential separations between the oxidation and reduction peaks were ca. 190 mV for both **1a** and **1b** (ca. 150 mV for the corresponding **3**). Differential pulse voltammetry was applied to the oxidation process of the diaminostilbenes **1**. Figure 2 displayed two oxidation responses ascribed to the two amine sites (potential difference of ca. 0.1 V). Cation-cation repulsion through the  $\pi$ -conjugation and/or steric closeness in the stilbene linkage of **1** separates the first and second oxidation steps of the amine sites.

The coulometric oxidation of **1b** under the application of 1.2 V with a carbon felt electrode was completed close to the electricity of two-equivalents for the **1b** molecule, and indicated the stoichiometric oxidation of the two amine sites (Fig. 3). The rotating-disk voltammetry of **1b** and **3b** was carried out under the same conditions to support the oxidation of **1** via a two-electron transfer reaction. The limiting current for **1b** was ca. 1.5-times larger than the one-electron oxidation current for **3b**. Plots of the limiting current vs. the square root of the rotation rate gave straight lines (inset in Fig. 3). The diffusion coefficients of **1b** and **3b** were estimated to be  $7.3 \times 10^{-6}$  and  $1.1 \times 10^{-5} \text{ cm}^2 \text{ s}^{-1}$ , respectively, by applying the Levich equation.<sup>12</sup> The ratio of the diffusion coefficients was approximately consistent with the inverse square-root value of the ratio of the molecular weights of **1b** and **3b**. This result supported the validity of the voltammetry and the two-electron oxidation of **1b** to form the biradical **2b**.

**Spectral Analysis.**  $\text{NOBF}_4$  was selected as the oxidizing agent to accomplish the chemical oxidation of **1**. The  $\text{CH}_2\text{Cl}_2$  solution of the diaminostilbene **1** was titrated with

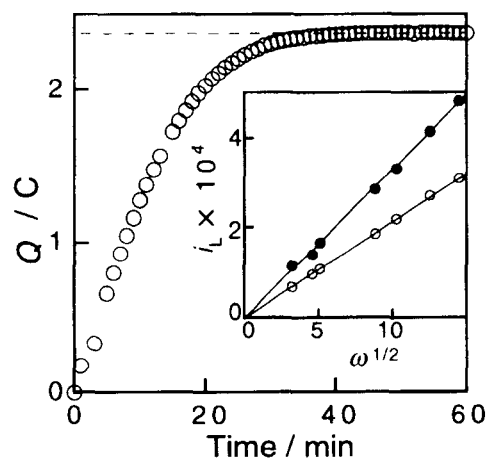


Fig. 3. Controlled potential coulometric oxidation of the diaminostilbene **1b** ( $1.23 \times 10^{-5}$  mol) in  $\text{CH}_2\text{Cl}_2$ . The dashed line is the theoretical quantity of electricity for stoichiometric oxidation ( $Q = 2.37 \text{ C}$ ). Inset: Plots of limiting current vs. square root of rate ( $\omega$ ) for **1b** (●) and **3b** (○).

a  $\text{CH}_2\text{Cl}_2$  solution of  $\text{NOBF}_4$  solubilized with 18-crown-6, and the oxidation was first monitored via its UV/vis spectrum. The  $\text{CH}_2\text{Cl}_2$  solution of **1** turned deep blue through the oxidation, being accompanied by a new absorption ( $\lambda_{\text{max}} = 689$  and 769 nm for **1a** and **1b**, respectively) which is characteristic of triphenylaminium cation radicals<sup>13</sup> (Fig. 4). This spectral change in the UV/vis region had an isosbetic point (at 332 and 345 nm for **1a** and **1b**, respectively), which could negate any side reaction during the oxidation. A small excess addition (ca. 0.4 equivalent excess) of  $\text{NOBF}_4$  to the amine site resulted in the formation of the biradical **2**, which was judged by the saturations of the visible absorption and ESR signal intensity mentioned below.

The oxidation of **1** with  $\text{NOBF}_4$  was accompanied by an increase in the ESR signal. The ESR spectra of the radicals **1a** and **1b** with low spin concentrations gave five-line signals (Fig. 5a) ascribed to the hyperfine coupling with two nitrogen

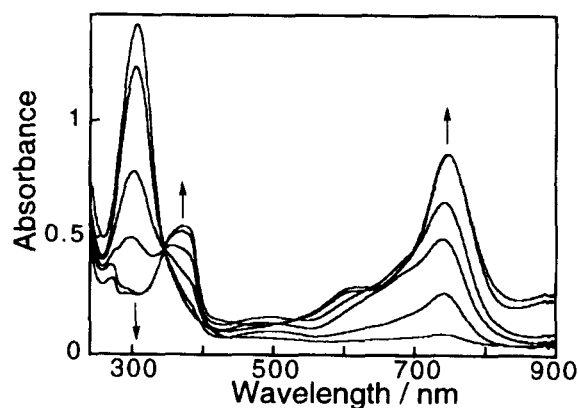


Fig. 4. UV/vis spectra of **1b** during the oxidation with  $\text{NOBF}_4$ .  $[\text{NOBF}_4]/[\mathbf{1b}] = 0.35, 0.70, 0.90, 1.05, \text{ and } 1.40$ .  $[\mathbf{1b}] = 0.2 \text{ mM}$  in  $\text{CH}_2\text{Cl}_2$ .

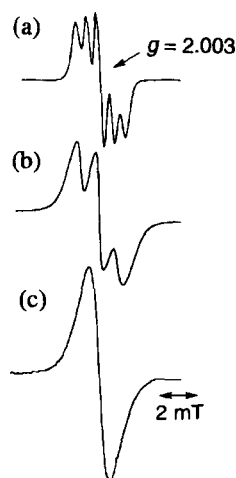


Fig. 5. ESR spectra of the cation radical **2b** in  $\text{CH}_2\text{Cl}_2$  at room temperature (a) **2b** with a spin concentration of 0.05 spin/amine unit, (b) spin concentration 0.45 spin/amine unit, and (c) spin concentration 0.90 spin/amine unit, respectively.

nuclei at  $g = 2.0026$  and  $2.0032$ , respectively. These spectra successively changed to three-line and unimodal signals (Figs. 5b and 5c) with increasing spin concentration, which was ascribed to an exchange broadening. The spin concentration reached 0.66 and 0.90 spin/amine unit for **2b** and **2a**, respectively, under the same oxidizing conditions. The half-life of the radical **2b** estimated by the ESR signal was ca. 7 d, even at room temperature, in the solid state **2b** dispersed in diamagnetic polystyrene.

The ESR spectra of the mono(cation radical) **3** gave hyperfine structures attributed to the two kinds of protons bound to the phenylene rings and hyperconjugation based on the protons of the *p*-substituted groups. For example, Fig. 6 shows the ESR spectrum for the radical **3a**, which has already been reported<sup>14</sup> but not yet described in detail. The experimental and simulated spectra using the coupling constants given in Table 1 were in fair agreement. The coupling constant,  $a_N$ , on the nitrogen atom was estimated to be 0.960 and 0.846 mT for **3a** and **3b**, respectively, which suggested that the spin

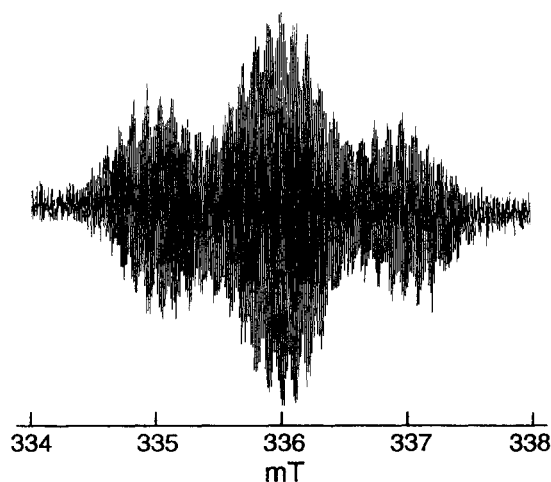


Fig. 6. ESR spectrum for the oxidation product of **3a** in  $\text{CH}_2\text{Cl}_2$  with  $\text{NOBF}_4$  at room temperature.

Table 1. Coupling Constants in the ESR Hyperfine Structure for the Triarylammonium Cation Radicals from **3**

	$a_N$	$a_{o-H}$	$a_{m-H}$	$a_{H(i-butyl \text{ or } methoxy)}$
<b>3a</b>	0.960	0.200	0.100	0.014
<b>3b</b>	0.846	0.183	0.061	0.061

density of **3b** was more delocalized over the entire molecule compared to **3a**. On the other hand, the  $a_{o-H}$  and  $a_{m-H}$  values on the *N*-substituted phenylene rings suggested a larger spin density polarization for **3a**.

The frozen  $\text{CH}_2\text{Cl}_2$  glass of a 10 mM ( $1 \text{ M} = 1 \text{ mol dm}^{-3}$ ) **2** with a high spin concentration gave a  $\Delta M_s = \pm 2$  forbidden transition at  $g = 4$  ascribed to a triplet species (insert in Fig. 7). The doubly integrated signal intensities of the transition for **2a** and **2b** obeyed Curie's law in the temperature range of 5–100 K (Fig. 7). However, no fine structure that gave the zero-field splitting parameters was detected.

**Magnetic Property.** Magnetization and static magnetic susceptibility of the biradicals **2a** and **2b** were measured using a SQUID magnetometer. Polystyrene was used as a diamagnetic diluent of the biradicals to minimize any inter-

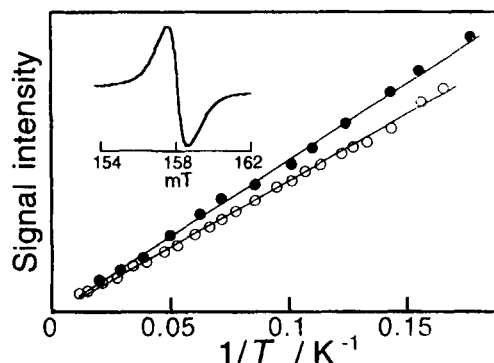


Fig. 7. Curie plots for the peak in the ESR  $\Delta M_s = \pm 2$  region for **2a** (○) and **2b** (●) with spin concentration = 0.66 and 0.90 spin/amine unit, respectively. Inset:  $\Delta M_s = \pm 2$  spectrum for **2a**.

molecular interactions. The magnetization ( $M$ ) normalized by the saturated magnetization ( $M_s$ ),  $M/M_s$ , is known to be represented by a Brillouin function. The  $M/M_s$  of **2a** is plotted vs. the effective temperature ( $T-\theta$ ) and compared with the Brillouin curves (Fig. 8a);  $\theta$  is the mean field parameter for small intermolecular magnetic interactions, and was estimated by referring to the literature.<sup>15</sup> The  $M/M_s$  plots were presented between the theoretical Brillouin curves for  $S = 1/2$  and  $2/2$  at 1.8–20 K, indicating a triplet ground state of the biradical.

The ratio of the effective magnetic moments ( $\mu_{\text{eff}}$ ) and the Bohr magneton ( $\mu_B$ ),  $\mu_{\text{eff}}/\mu_B$ , was shown in Fig. 9. The  $\mu_{\text{eff}}/\mu_B$  values of **2a** were almost constant in the range 20–200 K, or even at the higher temperature, as compared with, e.g., those of the corresponding 3,4'-bis(phenoxy) radical)-substituted stilbene. The latter behaved as two independent free radicals at higher temperature, and its  $\mu_{\text{eff}}/\mu_B$  increased with decreasing temperature ( $< 80$  K), indicating the ferromagnetic interaction (the triplet–singlet energy gap of ca. 50  $\text{cm}^{-1}$ ).<sup>16</sup> This result suggests that the triplet state is either the ground state stabilized from the singlet state with an energy gap greater than  $kT$ , or is degenerated with the singlet state for **2a**. The plots were located at the intermediate between  $\mu_{\text{eff}}/\mu_B = 2.45$  and 2.83 for  $S = 1/2$  and 1, respectively.

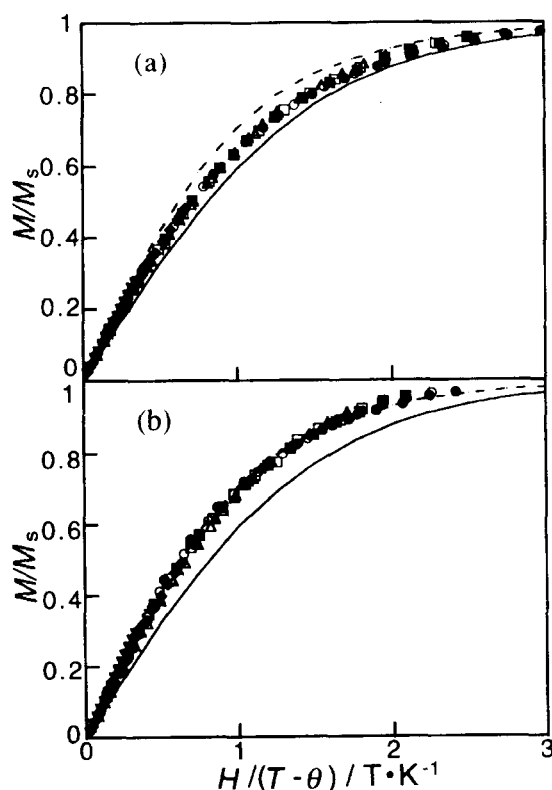


Fig. 8. Normalized plots of magnetization ( $M/M_s$ ) vs. the ratio of magnetic field and temperature ( $H/(T-\theta)$ ) for the biradical **2a** (a) and **2b** (b) with spin concentration 0.18 and 0.50 spin/amine unit, respectively. Powder samples diluted with polystyrene.  $T = 1.8$  (●), 2 (○), 2.25 (■), 2.5 (□), 3 (▲), 5 (△), 10 (◆), 15 (◇), 20 (▼) K and theoretical curves corresponding to the  $S = 1/2$  and  $2/2$  Brillouin functions.

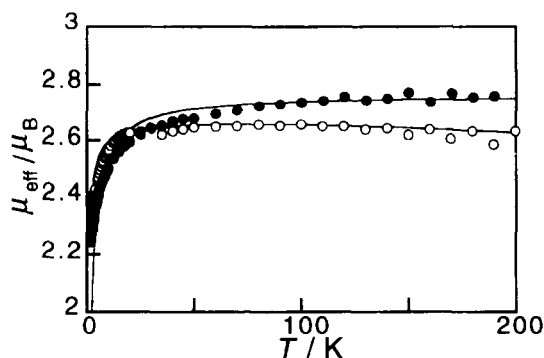


Fig. 9. The ratio of the effective magnetic moment and the Bohr magneton ( $\mu_{\text{eff}}/\mu_B$ ) vs. temperature ( $T$ ) plots of the biradical **2a** (○) and **2b** (●). Solid lines are the simulated curves calculated using the Bleaney–Bowers expression with the parameters  $x_1 = 0.45$ ,  $\theta = -0.55$  K, and  $J \gg kT$  for **2a** and  $x_1 = 0.30$ ,  $\theta = -1.1$  K, and  $J \gg kT$  for **2b**, respectively.

The value (ca. 2.6) could be reduced by the still low spin concentration which was determined by the saturated magnetization. These indicate that **2a** has a triplet ground state stabilized from the singlet state with an energy gap greater than  $kT$ . The  $\mu_{\text{eff}}/\mu_B$  decreased below 20 K, probably because of an intermolecular antiferromagnetic interaction.

The Bleaney–Bowers expression<sup>17</sup> is known for the analysis of the magnetic susceptibility in biradicals. The magnetic susceptibility of incomplete spin generation samples, such as **2**, would be expressed by the sum of the complete biradical fraction ( $1-x_1$ ) and the doublet monoradical fraction ( $x_1$ ). The modified expression is

$$\mu_{\text{eff}}/\mu_B = \left( \frac{6g^2T}{(T-\theta)(3 + \exp(-2J/kT))} (1-x_1) + \frac{3g^2T}{2(T-\theta)} x_1 \right)^{1/2}, \quad (1)$$

where  $J$  is the spin exchange coupling constant, which is positive for ferromagnetic coupling. Curve fitting of the  $\mu_{\text{eff}}/\mu_B$  data for **2a** in Fig. 9 to Eq. 1 yielded  $x_1 = 0.45$ ,  $\theta = -0.55$  K, and  $J > kT$ . The monoradical fraction is consistent with the magnetization plots located between  $S = 1/2$  and  $2/2$ .

The  $M/M_s$  plots for the powder sample of **2b** were almost on the curve of  $S = 2/2$  at 1.8–20 K, indicating a triplet ground state (Fig. 8b). The higher spin concentration of **2b** seemed to bring about a smaller monoradical fraction, compared with **2a**. Figure 9 also showed the  $\mu_{\text{eff}}/\mu_B$  data for **2b**; the plots were close to 2.83, even at the higher temperature. The stability of the triplet ground state ( $2J$ ) was estimated to be significantly large ( $\gg kT$ ) for the biradical **2**.

The 3,4'-disubstituted stilbene skeleton acted as an effective ferromagnetic coupler to connect the diphenylaminium cation radicals. Poly(cation radical)s derived from the 3,4'-bis(diarylamino)stilbenoid units are expected to show a strong intramolecular ferromagnetic coupling.

### Experimental

Bis(4-*t*-butylphenyl)amine **4a** was prepared by the reaction of 1-bromo-4-*t*-butylbenzene (4.7 g, 22 mmol) and 4-*t*-butylaniline (3.2 g, 21 mmol) in the presence of tris(dibenzylideneacetone)-

dipalladium (0.51 g, 0.56 mmol), BINAP (1.0 g, 1.6 mmol), and sodium *t*-butoxide (6.2 g, 65 mmol) for 18 h at 110 °C. Yield 82%; mp 111 °C (mp 107–108 °C in the lit.<sup>18</sup>). Bis(4-methoxyphenyl)-amine **4b** was prepared from 4-bromoanisole and 4-methoxyaniline. Yield 78%; mp 105 °C (mp 103 °C in the lit.<sup>19</sup>).

Tris(4-*t*-butylphenyl)amine **3a** was prepared by the reaction of 1-bromo-4-*t*-butylbenzene (0.53 g, 2.5 mmol) and bis(4-*t*-butylphenyl)amine (0.68 g, 2.4 mmol) in the presence of tris(dibenzylideneacetone)dipalladium (31 mg, 0.0034 mmol), tri-*o*-tolylphosphine (54 mg, 0.18 mmol), and sodium *t*-butoxide (6.2 g, 65 mmol) for 18 h at 100 °C. Yield 90%; mp 269 °C (mp 265 °C in the lit.<sup>20</sup>). Tris(4-methoxyphenyl)amine **3b** was prepared from 1-bromo-4-methoxybenzene and bis(4-methoxyphenyl)amine. Yield 70%; mp 93 °C (mp 94.5 °C in the lit.<sup>21</sup>).

3,4'-Dibromostilbene was prepared as follows. A volume of palladium(II) acetate (0.14 g, 0.62 mmol), tri-*o*-tolylphosphine (0.37 g, 1.2 mmol), and triethylamine (15 g, 0.15 mol) were added to 30 ml of an acetonitrile solution containing 3-bromostyrene (5.6 g, 31 mmol) and 1-bromo-4-iodobenzene (8.7 g, 31 mmol) under a nitrogen atmosphere, and the solution was then stirred for 14 h at 55 °C. The solution was evaporated, washed with 10% aqueous hydrochloric acid, and extracted with chloroform. After drying over anhydrous sodium sulfate, the solution was evaporated and developed on a silica-gel column with a hexane/chloroform (1/1) eluent. Yield 75%; mp 90 °C (mp 88 °C in the lit.<sup>3c</sup>).

**3,4'-Bis[bis(*p*-*t*-butylphenyl)amino]stilbene 1a.** 3,4'-Dibromostilbene (0.59 g, 1.7 mmol) and bis(4-*t*-butylphenyl)amine (1.0 g, 3.6 mmol) were dissolved in 13 ml of toluene. Sodium *t*-butoxide (0.54 g, 5.6 mmol), tris(dibenzylideneacetone)dipalladium (46 mg, 0.051 mmol), and tri-*o*-tolylphosphine (77 mg, 0.25 mmol) were added to the solution, and the reaction mixture was heated at 100 °C for 19 h under nitrogen. After cooling to room temperature, the resulting solution was quenched by adding aqueous ammonia (15 ml) and taken up in chloroform. The crude product was purified by flash chromatography on silica-gel using a hexane/chloroform (2/1) eluent to afford 1.1 g of **1a** as a green-yellow solid. Yield 88%; mp 235 °C; IR (KBr pellet) 1322 ( $\nu_{C-N}$ ), 959  $\text{cm}^{-1}$  ( $\delta_{transCH=CH}$ ); <sup>1</sup>H NMR (CDCl<sub>3</sub>, 500 MHz)  $\delta$  = 1.28 (s, 18H, *t*-butyl), 1.30 (s, 18H, *t*-butyl), 6.84–7.30 (m, 26H, ArH and –CH=CH–); <sup>13</sup>C NMR (CDCl<sub>3</sub>)  $\delta$  = 31.44, 31.46, 34.26, 34.28, 119.82, 121.70, 122.61, 122.72, 123.70, 124.09, 125.99, 126.03, 126.60, 127.19, 128.36, 129.27, 130.72, 138.75, 144.84, 145.15, 145.41, 145.82, 147.69, 148.47; MS  $m/z$  739 (M<sup>+</sup>). Found: C, 87.6; H, 8.4; N, 4.0%. Calcd for C<sub>54</sub>H<sub>62</sub>N<sub>2</sub>: C, 87.7; H, 8.5; N, 3.8%.

**3,4'-Bis[bis(*p*-methoxyphenyl)amino]stilbene 1b:** Yield 80%; mp 70 °C; IR (KBr pellet) 1320 ( $\nu_{C-N}$ ), 1242, 1036 ( $\nu_{O-C}$ ), 963  $\text{cm}^{-1}$  ( $\delta_{transHC=CH}$ ); <sup>1</sup>H NMR (CDCl<sub>3</sub>, 600 MHz, <sup>1</sup>H-<sup>1</sup>H COSY cross-peaks in aryl region)  $\delta$  = 3.79 (s, 6H, –OCH<sub>3</sub>), 3.80 (s, 6H, –OCH<sub>3</sub>), 6.78 (dd, 1H, *J* = 4, 8 Hz, 6.81–6.83, 7.13), 6.80 (d, 1H, *J* = 17 Hz, 6.89), 6.81–6.83 (overlapped, 8H, 7.03–7.06), 6.87 (d, 2H, *J* = 8 Hz, 7.25), 6.89 (d, 1H, *J* = 17 Hz, 6.80), 7.02 (d, 1H, *J* = 8 Hz, 7.13), 7.03–7.06 (overlapped, 9H, 6.78, 6.81–6.83), 7.13 (t, 1H, *J* = 8 Hz, 6.78, 7.02), 7.25 (d, 2H, *J* = 8 Hz, 6.87); <sup>13</sup>C{<sup>1</sup>H} DEPT(135°) NMR (CDCl<sub>3</sub>): nonquaternary region, expected, 14 resonances; found, 13 resonances  $\delta$  = 55.48, 114.65, 114.68, 118.46, 119.13, 120.06, 120.46, 126.17, 126.33, 126.57, 127.18, 128.25, 129.14; quaternary region, expected, 8 resonances; found, 8 resonances  $\delta$  = 129.59 (q), 138.66 (q), 140.76 (q), 141.15 (q), 148.22 (q), 149.06 (q), 155.66 (q), 155.90 (q); MS  $m/z$  635 (M<sup>+</sup>). Found: C, 79.3; H, 6.3; N, 4.6%. Calcd for C<sub>42</sub>H<sub>38</sub>N<sub>2</sub>O<sub>4</sub>: C, 79.5; H, 6.0; N, 4.4%.

**Oxidation.** A CH<sub>2</sub>Cl<sub>2</sub> solution (0.10 ml) of **1** (2.0 mg) was

stirred for a few min with a CH<sub>2</sub>Cl<sub>2</sub> solution (0.50 ml) of NOBF<sub>4</sub> (1.7 mg) solubilized with 18-crown-6 (100 mg) in a glove box to yield the corresponding aminium cation radicals.

**Spectroscopic Measurements.** ESR spectra were taken on a JEOL JES-2XG ESR spectrometer with 100-kHz field modulation. The spin concentration of each sample was determined based on the assumption of *S* = 1/2 by careful integration of the ESR signal standardized with that of a TEMPO (2,2,6,6-tetramethyl-1-piperidinyloxy) solution.

The IR, NMR, mass, and UV/vis spectra were measured with a JASCO FT/IR-410, a JEOL NMR 500A or a Bruker NMR AVANCE-600, a Shimadzu GC-MS 17A, and a JASCO V-550 spectrometers, respectively. A 0.2 mm light-path length cell was used for the UV/vis measurements.

**Electrochemical Measurements.** Cyclic voltammetry and rotating-disk voltammetry were carried out with a platinum working electrode using a function generator (Nikko Keisoku NPG-3), potentiogalvanostat (NPGS-301), and motor speed controller (SC-5) at the scan rate of 100 and 5 mV s<sup>−1</sup>, respectively. The differential pulse voltammetry was carried out using an arbitrary function generator and potentiostat/galvanostat BAS 100B. For coulometry, a large carbon felt electrode was used with a digital coulomb meter (Nikko Keisoku DDCM-2). All of the electrochemical experiments were carried out in CH<sub>2</sub>Cl<sub>2</sub> in the presence of 0.1 M (*n*-C<sub>4</sub>H<sub>9</sub>)<sub>4</sub>NBF<sub>4</sub> as the supporting electrolyte.

**Magnetic Measurement.** A CH<sub>2</sub>Cl<sub>2</sub> solution of the biradical was immediately used after the oxidation. After removing the solvent, the neat sample was dissolved again in a CH<sub>2</sub>Cl<sub>2</sub> solution of polystyrene ([polystyrene]/[2] = 100 w/w). The solvent was thoroughly removed, and the resulting powder was transferred to a diamagnetic capsule for measurement. Magnetization and static magnetic susceptibility were measured with a Quantum Design MPMS-7 SQUID magnetometer. The magnetization was measured from 0.5 to 7 T at 1.8, 2, 2.25, 2.5, 3, 5, 10, 15, and 20 K. The static magnetic susceptibility was measured from 2 to 200 K in a field of 0.5 T. The ferromagnetic magnetization ascribed to impurities (< 10 ppm) was determined by the Honda–Owen plots and subtracted from the overall magnetization. Diamagnetic susceptibility of the matrix and the capsule was estimated by the Curie plots of the magnetic susceptibility. The corrected magnetization data were fitted to Brillouin functions using a self-consistent version of the mean field approximation.

This work was partially supported by a Grant-in-Aid for Scientific Research No. 09305060 from the Ministry of Education, Science and Culture and by the NEDO Project on Technology for Novel High-Functional Materials.

## References

- Reviews: a) A. Rajca, *Chem. Rev.*, **94**, 871 (1994). b) J. S. Miller and A. J. Epstein, *Angew. Chem., Int. Ed. Engl.*, **33**, 385 (1994). c) K. Matsuda, K. Inoue, N. Koga, and H. Iwamura, *Bull. Chem. Soc. Jpn.*, **69**, 1483 (1996). d) P. M. Lahti, "Magnetic Properties of Organic Materials," Marcel Dekker, New York (1999). e) K. Itoh, "Molecular Magnetism," Kohdansha Scientific, Tokyo (1999).
- Recent papers: a) J. Sedó, N. Ventosa, D. Ruiz-Molina, M. Mas, E. Molins, C. Rovira, and J. Veciana, *Angew. Chem., Int. Ed. Engl.*, **37**, 330 (1998). b) A. Rajca, J. Wongsriratanakul, S. Rajca, and R. Cerny, *Angew. Chem., Int. Ed. Engl.*, **37**, 1229 (1998). c)

- H. Nishide, M. Miyasaka, and E. Tsuchida, *Angew. Chem., Int. Ed. Engl.*, **37**, 2400 (1998). d) H. Nishide, M. Miyasaka, and E. Tsuchida, *J. Org. Chem.*, **63**, 7399 (1998). e) K. K. Anderson and D. A. Dougherty, *Adv. Mater.*, **10**, 688 (1998). f) A. Rajca, S. Rajca, and J. Wongsriratanakul, *J. Am. Chem. Soc.*, **121**, 6308 (1999). g) T. Itoh, K. Matsuda, and H. Iwamura, *Angew. Chem., Int. Ed. Engl.*, **38**, 1791 (1999). h) Y. Pu, M. Takahashi, E. Tsuchida, and H. Nishide, *Chem. Lett.*, **1999**, 161.
- 3 a) K. Mukai, *Bull. Chem. Soc. Jpn.*, **48**, 2405 (1975). b) J. Veciana, C. Rovira, M. I. Crespo, O. Armet, V. M. Domingo, and F. Palacio, *J. Am. Chem. Soc.*, **113**, 2552 (1991). c) N. Yoshioka, P.M. Lahti, T. Kaneko, Y. Kuzumaki, E. Tsuchida, and H. Nishide, *J. Org. Chem.*, **59**, 4272 (1994). d) A. Rajca and S. Rajca, *J. Am. Chem. Soc.*, **118**, 8121 (1996). e) R. J. Bushby, D. R. McGill, K. M. Ng, and N. Taylor, *J. Chem. Soc., Perkin Trans. 2*, **1997**, 1405. f) K. Hamachi, K. Matsuda, T. Itoh, and H. Iwamura, *Bull. Chem. Soc. Jpn.*, **71**, 2937 (1998). g) J. A. E. H. van Haare, M. van Bostel, and R. A. J. Janssen, *Chem. Mater.*, **10**, 1166 (1998).
- 4 a) R. I. Walter, *J. Am. Chem. Soc.*, **77**, 5999 (1955). b) E. T. Seo, R. F. Nelson, J. M. Fitch, L. S. Marcoux, D. W. Leedy, and R. N. Adams, *J. Am. Chem. Soc.*, **88**, 3498 (1966). c) L. Hagopian, K. Günter, and R. I. Walter, *J. Phys. Chem.*, **71**, 2290 (1967). d) S. Sasaki and M. Iyoda, *Chem. Lett.*, **1995**, 1011.
- 5 a) K. Yoshizawa, A. Chano, A. Ito, K. Tanaka, T. Yamabe, H. Fujita, and J. Yamauchi, *Chem. Lett.*, **1992**, 369. b) K. Yoshizawa, A. Chano, A. Ito, K. Tanaka, T. Yamabe, H. Fujita, J. Yamauchi, and M. Shiro, *J. Am. Chem. Soc.*, **114**, 5994 (1992). c) K. R. Stickley and S. C. Blackstock, *J. Am. Chem. Soc.*, **116**, 11576 (1994). d) K. R. Stickley and S. C. Blackstock, *Tetrahedron Lett.*, **36**, 1585 (1995). e) M. Yano, M. Furuichi, K. Sato, D. Shiomi, A. Ichimura, K. Abe, T. Takui, and K. Itoh, *Synth. Met.*, **85**, 1665 (1997).
- 6 K. Sato, M. Yano, M. Furuichi, D. Shiomi, T. Takui, K. Abe, K. Itoh, A. Highchi, K. Katsuma, and Y. Shirota, *J. Am. Chem. Soc.*, **119**, 6607 (1997).
- 7 R. J. Bushby and D. Gooding, *J. Chem. Soc., Perkin Trans. 2*, **1998**, 1069.
- 8 Preliminary communication of this paper: T. Michinobu, M. Takahashi, E. Tsuchida, and H. Nishide, *Chem. Mater.*, **11**, 1969 (1999).
- 9 a) J. Louie and J. F. Hartwig, *J. Am. Chem. Soc.*, **119**, 11695 (1997). b) J. Louie and J. F. Hartwig, *Macromolecules*, **31**, 6737 (1998).
- 10 G. Märkl and A. Merz, *Synthesis*, **1973**, 295.
- 11 a) F. D. King and D. R. M. Walton, *J. Chem. Soc., Chem. Commun.*, **1974**, 256. b) P. Strohmriegel, G. Jesberger, J. Heinze, and T. Moll, *Makromol. Chem.*, **193**, 909 (1992).
- 12 A. J. Bard and L. R. Faulker, "Electrochemical Methods," Wiley, New York (1980).
- 13 a) F. A. Neugebauer, S. Bamberger, and W. R. Groh, *Chem. Ber.*, **108**, 2406 (1975). b) W. Schmidt and E. Steckhan, *Chem. Ber.*, **113**, 577 (1980).
- 14 G. A. Pearson, M. Rocek, and R. I. Walter, *J. Phys. Chem.*, **82**, 1185 (1978).
- 15 a) J. Veciana, C. Rovira, N. Ventosa, M. I. Crespo, and F. Palacio, *J. Am. Chem. Soc.*, **115**, 57 (1993). b) N. Fukita, M. Ohba, H. Okawa, K. Matsuda, and H. Iwamura, *Inorg. Chem.*, **37**, 842 (1998).
- 16 H. Nishide, T. Kaneko, T. Nii, K. Katoh, E. Tsuchida, and P. M. Lahti, *J. Am. Chem. Soc.*, **118**, 9695 (1996).
- 17 B. Bleaney and K. D. Bowers, *Proc. R. Soc. London, Ser. A*, **214**, 451 (1952).
- 18 D. Craig, *J. Am. Chem. Soc.*, **57**, 195 (1935).
- 19 H. Wieland, *Ber. Dtsch. Chem. Ges.*, **41**, 3493 (1908).
- 20 R. I. Walter, *U. S. Dept. Com., Office Tech. Serv., PB Rept.*, **154, 498**, 63 (1960); *Chem. Abstr.*, **59**, 416d (1963).
- 21 H. Wieland and E. Wecker, *Ber. Dtsch. Chem. Ges.*, **43**, 705 (1910).